NASA-TM-77025 19840007050

A Reproduced Copy

OF

NASA TM-77025

Reproduced for NASA

by the

NASA Scientific and Technical Information Facility

FFNo 672 Aug 65

THREE-DIMENSIONAL EFFECTS ON AIRFOILS

J. P. Chevallier

N84-15118

1. Report No. NASA TM-77025	2. Government Accession No.	3. Recipient's Catalog No.
4. Title and Subtitle THREE-DIMENSIONAL EFFECTS ON AIRFOILS		5. Report Date February 1983
		6. Performing Organization Code
7. Author(s) J. P. Chevallier		8. Performing Organization Report No.
		10. Work Unit No.
9. Performing Organization Name and Address SCITRAN Box 5456 Santa Barbara, CA 93108		11. Contract or Grant No. NASw 3542
		13. Type of Report and Period Covered Translation
12. Sponsoring Agency Name and Address National Aeronautics and Space Administration Washington, D.C. 20546		14. Sponsoring Agency Code

15. Supplementary Notes

Translation of "Effets tridimensionnels sur les profils)"
Office National D'Etudes et de Recherches Aerospatiales,
Chatillon (France), ONERA-TP-1981-117 (Presented at 18th
Colloquim on Applied Dynamics, Association Aeronautique
et Astronomie de France, Poiters, Nov. 18-20, 1981) 1981, pp. 1-34.
(A82-19734)

16. Abstract The transonic flow field computer program assessment,
recommended by the GARTEur action groups, requires a good
knowledge of the experimental conditions for two-dimensional
tests used as a validation base.
    Besides the conventional wall effects, now conveniently
corrected, the three-dimensional effects, mainly due to the
boundary layers on the walls at the ends of an airfoil spanning
the working section are demonstrated by some tests in the sub
and transonic speed range. These effects are so important that
their minimization is suitable and a good modelization is re-
quired to be sure of their correction. A critical survey of
modelizations compared to experimental results leads to the
conclusion that a refined and realistic analysis is needed to
improve corrections applied to the test results.

17. Key Words (Selected by Author(s))	18. Distribution Statement Unlimited		
19. Security Classif. (of this report) Unclassified	20. Security Classif. (of this page) Unclassified	21. No. of Pages 44	22. Price

SUMMARY

The transonic flow field computer program assessment, recommended by the GARTEur action groups, requires a good knowledge of the experimental conditions for two-dimensional tests used as a validation base.

Besides the conventional wall effects, now conveniently corrected, the three-dimensional effects, mainly due to the boundary layers on the walls at the ends of an airfoil spanning the working section are demonstrated by some tests in the sub and transonic speed range. These effects are so important that their minimization is suitable and a good modelization is required to be sure of their correction. A critical survey of modelizations compared to experimental results leads to the conclusion that a refined and realistic analysis is needed to improve corrections applied to the test results.

NOTATIONS

A : geometrical aspect ratio

b, B : half-size and size of the test section

c : airfoil chord

C_p : pressure coefficient

C_A, C_N, C_x, C_y : aerodynamic coefficients for local axial, normal, drag and lift forces

H : shape factor of the boundary layer

k : factor of influence of the lateral boundary layers

M : Mach number

R_e : Reynolds number

s : clearance between model and wall

U : local speed in the boundary layer

x, y : longitudinal and transversal coordinates

α : angle of attack

β : compressibility factor

Γ : circulation

$\delta, \delta_1, \delta_2$: thickness, displacement thickness and momentum thickness of the boundary layers.

OFFICE NATIONAL D'ETUDES ET DE RECHERCHES AEROSPATIALES

THREE DIMENSIONAL EFFECTS ON AIRFOILS
J.P. Chevallier

1 - INTRODUCTION

The development of calculation means and methods, in the   /2*
relatively simple case of two-dimensional flows, should soon
make it possible to limit the use of tests in airfoil inves-
tigations. A cogent comparison with experimental results,
however, will still be useful for validating theoretical re-
sults. Such a comparison is the purpose of the computer pro-
gram assessment, recommended in 1980 by the GARTEur** action
groups AG 02 and 05. Its success depends on whether we can be
sure of the validity of the two-dimensional tests. In a pre-
liminary phase, a series of results obtained in various wind
tunnels had been gathered [1] to serve as a data base. Owing
to the diversity of the test conditions, their coherence may
be assured only if the various interferences are suitably cor-
rected. The effect of the boundary conditions on the upper ·
and lower walls may at present be considered to be the most
important one and theoretically the best known one, provided
that all measurements used for determining the modulus refer-   /3
ence speed and direction are performed with sufficient accur-
acy on a control surface near the boundaries of the fluid
test section in the vicinity of the model.

Conversely, the two-dimensionality hypothesis of the flow
must be carefully checked, because it is too often implicitly
assumed in wind tunnels with adaptable walls as well as in con-
ventional installations. To encourage such checks, we shall

---

*Numbers in the margin indicate pagination in the original text.
**Group for Aeronautical Research and Technology in Europe. ...

demonstrate on a few examples that airfoil tests exhibit three
dimensional effects that are often quite significant in terms
of current accuracy expectations. These three-dimensional ef-
fects, mainly arising from the boundary layers on the side
walls in the presence of an airfoil, were detected a long time
ago and models [2] have been formed of them in order to calcu-
late the corrections. A few experimental studies have been
carried out on them, but the results are not consistent enough
to establish simple correction formulas and the purpose of the
present report is to make designers and experimenters aware of
the uncertainties of the test results.

Typical examples in the sub and transonic speed range will
be presented first. The main modelizations will then be examin-
ed. An attempt will then be made to bring out the main points
used to assess their validity, but it will remain very diffi-
cult to draw conclusions.

2 - EXAMPLES OF AIRFOIL TESTS BETWEEN WALLS

The most common method of testing plane currents is to
use a rectangular test section: the airfoil under study is at-
tached between two walls (that we will call lateral or side
walls) on an angle-of attack setting device, or a balance.
This assembly allows for a large number of pressure intake
tubes used to record distributions over one or several sections.

2.1 - Tests Offering An Analysis Along the Span

Use of a model sliding sideways in a slot cut out on the
wall offers a fine study of pressure distributions in the
boundary layer.

A. Caillou [3] used this technique for a Clark Y airfoil
with a 150 mm chord and 250 mm span in the presence of

2

a boundary layer with a conventional thickness of 7.5 mm at the leading edge of the model. The pressure distributions on the airfoil were recorded for angles of attack α of -3°/0/3/6 and 9° and for distances from the wall of 0.6/1.6/2.6/3.6/6.6 and 8.6 mm. Reproduced for illustration for 6° in figure 1, they already make it possible to conclude that they are very similar to the distributions recorded concurrently in the central section. If it is not permitted to speak of circulation in the plane of the wall, we can say that the local lift coefficient C_z obtained by the pressure integral is virtually constant along the span (figure 2).

H.A. Dambrink [4] did similar work in a 0.55 x 0.42 m transonic wind tunnel on a model with a chord of 180 mm and a span of 420 mm in the presence of a 21 mm boundary layer and for angle of attacks of 0.35/3.6 and 5,8° for Mach numbers of 0.3/0.5/0.7 and 0.84. The pressure distributions are taken for fewer distances from the wall in the boundary layer, but for more complete ones outside of it. Extracts from these results given in figure 3 confirm the preceding conclusions pertaining to the reductions in distribution points and to the fact that the general speed level had decreased (although to a less extent) on the lower surface and upper surface, while a local variation of the circulation would have the opposite effects on the two sides of the airfoil. Furthermore, if we consider the factors of resistance to forward motion (figure 4) obtained by integrating the pressures, we find that they increase in the vicinity of the wall, while the lift slightly decreases. The hypothesis of a simple modification of the angle of attack in the boundary layer cannot explain these two effects which appear at a distance from the wall equal to about five times the boundary layer thickness. Under these conditions, it is normal that the overall measurements of airfoil effects give considerably different results for the airfoild drag than those obtained from the pressure integrals at the center of the test section of slipstreams.

Furthermore, the supersonic region is the center of a local interference at supercritical Mach numbers: the weak shock produced at top speeds, and therefore in a sharp recompression gradient, is likely to cause a considerable thickening of the lateral boundary layer (figure 5). The existence of this type of interference is confirmed in other tests [5] using visualizations (figure 6) which clearly show traces of a weak shock issuing from the lateral wall in the laminar and locally supersonic region. The origin of this interference in this case no longer seems to be associated with a strong recompression gradient, as this modern airfoil presents a very flat pressure distribution on the upper surface (figure 7).

The shock appearing on this pressure distribution at about 40% from the central chord also leaves a visible trace (figure 6). The latter, however, has a consistent curved appearance and is slightly offset between the regions where the transition has, or has not yet, started. Without considering this offset, the two-dimensionality error at the shock position is about 0.1 c.

At low speeds, works of a more general scope have been undertaken on the effects of tip clearance of blading in the presence of a nonuniform flow [6]. The case of zero clearance is included and it appears as a perfectly normal boundary transition with respect to non zero clearances (figure 8). At a given span level, the boundary layer varies in increasing proportions (at 1.5 c upstream from the airfoil δ_1 increases from 0.4 mm to 3.8 mm). These variations are obtained either by extending the wall, or by action on a slot to eliminate the boundary layer. The local C_z in the median plane in this case do not vary in a manner which is consistent with the boundary layer thicknesses: figure 9.

Furthermore, in the event of a decrease in local lift in

4

the vicinity of the wall, the drag increases, at least up to distance of about δ . The abrupt and considerable decrease of C_x which appears for distances shorter than δ did not appear in Dambrink's investigation [4], figure 4.

A later work by Sugiyama demonstrated the effect of a given chord and boundary layer aspect ratio [7]. Excluding cases where the clearance is not zero, we retain only the curves shown in figure 10. The representation selected by the author, which correlates the positions of the measuring points with the span, which varies with the distance between the walls, shows that the boundary layer with a conventional thickness of 3.1 mm (measurement made at 1.5 chord upstream from the leading edge, δ_4 = 0.4 mm), corresponds to the variable values of ratio δ/b . This thickness is shown in figure 10. The lift distribution is more uniform as the width is thinner and as the lift increases.

For the study of the effects of a wing tip clearance, the author calculated the aspect ratio that accounts for the image of the model with respect to one of the walls alone (which is strange when the clearance is zero). Moreover, the results in this case are not perfectly symmetrical. The author's remarks on the overall results (at zero clearance) stress that the lift for the greatest aspect ratio is close to the expected values for truly two-dimensional flows. A C_y curve of the median section plotted as a function of δ/b from these results and extrapolated at $\delta = 0$ defines this trend (figure 11).

2.2 - Testing With Measurements in the Median Plane

Let us review the only experiments in which, to our knowledge, the thickness of the side wall boundary layer is varied alone in the presence of airfoils with different chords. These results were presented by Bernard Guelle [8] in 1975 at

Poitiers and in 1977 [9]. Unfortunately, they do not include
an analysis along the span of the model, but only the measure-
ment of the pressures on its median section. We could also
regret that the small width of the windtunnel does not allow
a large enough domain to be covered for ratios δ_1/b always
greater than 0.01, and $c/_{2b}$ greater than 0.75.

They nevertheless make it possible to show that, in the
median plane of the windtunnel, everything happens as if the
airfoil were subjected to a deflected stream with an angle $\Delta\alpha$
proportional to the airfoil lift (or to the angle of attack α
with repsect to the direction of zero lift) and that the coef-
ficient of porportionality itself was proportional to the
boundary layer thickness. A relatively constant factor of
influence was therefore defined by $k = \frac{\Delta\alpha}{\alpha} \cdot \frac{b}{\delta_1}$.

The residual variations of this factor as a function of
the Mach number for various airfoils of various chords and
for several angles of attack are given in figure 12. They
shown that, if a rough mean value of 1.5 may be assumed for
any value below a critical Mach number, large and complex
variations appear at higher Mach numbers.

In the studies reviewed up to here, the angles of attack
do not reach values at which large separations may be detected.
This is obviously no longer the case for tests carried out on
lift augmented airfoils. The performance limits of devices
used to increase the maximum lift (nose, flaps, ...) are a func-
tion of the behavior of boundary layers in the presence of very
strong pressure gradients and these affect the boundary layers
of windtunnel walls more than those which originate on the ele-
ments of the model. A strong local suction of the lateral
boundary layers effectively corrects their ill-timed separation
[10].

6

As of 12° angle of attack, visualizations using strands
of wool (figure 13) clearly show that separations issuing from
either of the airfoil's tips contaminate any flow, whereas
with a reduction of the lateral boundary layers, the separa-
tion originates toward the trailing edge and in the median
region of the model for an angle of incidence close to 16°.
At a given angle of attack, the variation of the normal force
coefficents of each element of the lift augmented airfoil (nose,
body, flap) as a function of the lateral boundary layer suc-
tion rate defines an asymptotic trend validating this mode of
control (figure 14). The ratio of the values with maximum
suction to the values without suction are shown in the follow-
ing table for two angles of attack:

	Nose	Body	Flap
12°	1.45	1.15	0.71
18°	1.62	1.42	0.77

Beyond the separation point, the differences are enor-
mous, especially on the nose, where C_N increases about 50%.
Conversely, stresses on the flap decrease with a reduction of
the lateral boundary layers which suppress the acceleration
of the flow on the upper surface between the lateral separa-
tions.

These observations demonstrate the complexity of three-.
dimensional effects, which in this case obviously cannot be
aasimilated with a simple correction of the angle of attack,
even for the median section.

2.3 - Remarks On The Test Results

From the set of fairly disparate examples shown, two con-
clusions may be drawn on the three-dimensional effects in the
airfoil tests.

First, a nonuniformity appears on the span, either on the
lift and drag distributions deduced from the pressure integra-
tion, or on the shock positions. This nonuniformity extends
way beyond the boundary layer.

Second, even when the distribution is uniform on a large
central area of the span, its level is affected by a variation
fo the lateral boundary layer thicknesses.

To assess the significance of the first effect, a compar-
ison should be made of the variables involved, such as the
Mach number, the angle of attack or the nature of the boundary
layer (figure 15).

The shock position (detected on the pressure distributions)
at a given Mach number varies with the angle of attack and this
variation differs, depending on whether the boundary layer tran-
sition is natural or onset. The deviation of about 10% from
the chord of the positions observed by visualizations between
the central section and the ends therefore corresponds to an
angle of attack variation of nearly 1° and exceeds the transi-
tion onset effect.

In the presence of nonuniform distributions of the
characteristic studied (C_x , C_z , shock position) over the span,
if we focus our attention on the median section and try to
extrapolate the results as a function of a typical boundary
layer thickness, difficulties still appear.

Bernard Guelle [8] showed that, for the values of $\delta_1/_b$ available to him, a quasi-linear extrapolation could lead to relative values of $\delta_1 = 0$ (Figure 16). The use of the results of Sugiyama [7] with $0.005 < \delta_1/_h < 0.03$ (Figure 10) shows that this linearity cannot exist for very slight thicknesses of the boundary layer. Consideration of the influence coefficient k

$(-k = \frac{\Delta f}{f} \cdot \frac{b}{\delta_1})$ would then be of no interest or importance. However by giving values greater than those shown in [8] , which can be considered minimal in the evaluation of the errors, one can neglect the effects of the lateral boundary layers in the middle section.

By adopting a value on the order of 2 for k, it would appear that, even with a relatively thin boundary layer ($\delta_1/_b \approx 0,01$), the incidence correct is 2%.

Let us examine the consequences of such an error in the transition of the Lilienthal polar of Figure 17 (obtained by integration of the pressure on the NACA 0012 profile) to the Eiffel polar: for $\alpha = 8°$, we find, without the boundary layer, $C_N = 0.92$ and $C_A = 0.12$, or $C_x = 0,0092$. With a reduced C_N of 2% by the induced incidence, we obtain $C_x = 0,0066$ or $\Delta C_x = 0,0026$ and $\Delta C_x/_{C_x} = 39$ % . This relative error is exaggerated by the fact that consideration is only given to the pressure drag; any drag balance calculation would be illusory.

3 - MODELING OF LATERAL BOUNDARY LAYER EFFECTS

3.1 - Circulation Models

The oldest model [2] and also the most frequently used with several variations [12, 13, 14, 15] is that of Preston. It is first necessary to place it in context: In 1944

when Preston was about to set up an airfoil test section project, he wrote: "in a concern for energy-savings and the cost of machining the models, they must be as small as possible, yet large enough to permit accurate force measurements in the presence of boundary layers on the side wall".

His theroretical report providing an assessment of this minimum size begins with these words: "As a rough first approximation", ... As with any rough first approximation, it is assumed that in the region delimiting the wing's presence in the boundary layer, the local lift varies with U^L, U being the local speed at a certain distance from the wall, correlating this lift to circulation Γ, the latter becomes proportional to U and is reduced to zero at the wall.

The variation of circulation along the span creates a set of free half-unlimited vortices whose axes are parallel to the flow and that are localized in thickness δ. The speed profile in the boundary layer also gives the distribution of their intensity; they may therefore be replaced by an equivalent vortex of intensity Γ and located at a distance of displacement δ_1 /8 from the wall. Taking the first image of this vortex in the adjacent wall into account, Preston established the following simple formula:

$$\frac{\Delta\alpha}{\alpha} = \frac{4c\,\delta_1}{B^2} = \frac{\ell}{A}\cdot\frac{\delta_1}{b}$$

for the correction in the median plane.

The distribution along the span, calculated according to this scheme is compared in figure 19 with the scarce existing experimental results [11].

The same fundamental hypothesis of a variation of circulation proportional to the local speed in the boundary layer is retained by Menard [12] who accounts not only for the first

10

image of the longitudinal branches of the vortices, but the infinite line of alternating vortices corresponding to the successive images relative to the side walls.

He also explains the approximation made in [2] and [12] where the variations of circulation induced out of the boundary layers to determine the distribution of free vortices are negligible.

If we refer to figure 20 extracted from [12], the variations of the angle induced are of the order of the angle of attack itself (8°) and are therefore far from being negligible.

In the median section, by assuming that $\eta \, \delta_1$ is small in comparison with the side of test section B and that the lift is equal to $2 \pi \alpha$ we find:

$$\frac{\Delta \alpha}{\alpha} = \frac{\pi^2}{A} \cdot \frac{\delta_1}{b}$$

S. Schneider [14] improved this point by establishing and solving the integrodifferential equation (analogous to that of Prandtl) on the span that must be satisfied by the circulation distribution which is assumed to be proportional to the angle of attack and to the local speed.

As the successive images relative to the side walls are taken into consideration, the speed varies periodically on one wing whose span is unlimited and from this fact, it may be divided into a Fourier series to resolve the Prandtl equation, while the airfoil remains reduced to a lifting line.

Numerical results were obtained using an approached analytical representation of speed profiles in the boundary layers.

In a special case, they may be compared to the preceding formulas as far as the span-wise distribution of the rise of the wing center (figure 21) and for the effects on the median section (figure 22) as an inverse function of the geometric elongation.

A modification of the vortex scheme adopted by all preceding authors was propsed by Lazareff [15] while retaining the vortex associated with the lifting line. He assumed that the free vortices issue from the trailing edge of the airfoil and that, like the experiments, the lift is constant in the boundary layers. Figure 23 extracted from the document mentioned shows a correction of ΔC_z that is more uniform and slightly diminished, which corresponds well to the suppression of marginal vortices on 3/4 of the chord in the region closest to the lifting line.

The latter two analyses [14] [15] thus lead to fairly flat distributions over the span so that the totally different assumptions of the other modelizations do not seem too shocking.

3.2 - Non-Vortex Modelizations

Their common point lies in the observation that the experimental distributions of normal force being very flat, the assumption of a virtually flat flow may be retained and that the effect of the lateral boundary layers may be assimilated with that of the variations of their displacement thicknesses along the entire height of the test section. Qualitatively, the acceleration of the flow on the upper surface of the airfoil decreases the thickness of the lateral boundary layers (figure 27) and the resulting increase in the section slows down the acceleration and decreases the lift.

12

To obtain numerical results from this scheme, Barnwell [16] extracts the variations of displacement thickness of the lateral boundary layers (in the presence of the airfoil) from Karman's equation by introducing the empty test section values of the shape factor H and δ_1. The shape of the "small inter-ferences" given for the equation of flow conservation makes it possible for him to introduce a compressiblity factor $\bar{\beta}$ that includes the lateral boundary layer effects. His analysis of magnitudes that depend on $\bar{\beta}$ or β, respectively lead to an explicit formula for the lift loss:

$$\bar{c}_N / c_N = \frac{\sqrt{1 - M_\infty^2}}{\sqrt{1 - M_\infty^2} + (2 + H - M_\infty^2) 2 \Gamma_1 / \beta}$$

Another attempt based on analogous hypotheses, but not published owing to its nonrigorous nature [17] gives the value of the coefficient of influence in an even more simple form:

$$k = \frac{\Delta \alpha}{\alpha} \cdot \frac{b}{\delta_1} = \frac{H + 2 - M_\infty^2}{2(1 - M_\infty^2)}$$

The common point of these results is the disappearance of any effect from the chord (figure 23), the factor of influence depending little or not at all on δ_1 / b (figure 24), but varying noticeably with the Mach number (figure 12).

3.3 - Critique of the Modelizations

The modelizations were classed into two categories:

-the vortex schemes issuing from that of Preston;
-the nonvortex schemes where the span of the fluid test section

is considered in the presence of displacement thicknesses
modified by the airfoil field.

Independently of this classification, the critiques may
pertain to the base of the schematization, to the approxima-
tions made to develop a formulation and to the experimental
validations.

3.3.1 - Schematization Bases

The explanations given as a basis for the vortex scheme
are not very clear. Undoubtedly, in the case of a limited span,
a vortex cannot end in space, but nothing prevents it from end-
ing against a wall. Can the boundary layer that develops on
this wall prevent this? This is not obvious: although the
ground wind has a boundary layer profile on the ground and on
the sea, cyclones do not seem to be accompanied by a horizontal
vortex near this wall.

The justification given by Preston is based on the hypo-
thesis that, in the sections of the airfoil under the boundary
layer, the lift C_y varies with U^2 which the experiment stric-
tly prohibits (figure 2)..

In any case, if we could strictly justify this scheme, it
would be necessary to adopt the form proposed by Lazereff [15]
that eliminates the free vortex segment between the lifting
line and the trailing edge in conformity with the physical
conditions of the flow in this region where the tightness be-
tween model and wall prevent the establishment of a circula-
tic.- under the effect of lower surface and upper surface pres-
sure differences.

Moreover, we do not quite understand how the vortex could
originate beyond the trailing edge, where their equality be-
comes reestablished. Zonzero speeds with

14

opposite signs associated with a divergence or convergence of the flow may, on the other hand, create a vortex sheet in the slipstream.

The importance of the effects of a lateral clearance which precisely makes it possible to establish such a marginal circulation is illustrated by Sugiyama's experiments [6, 7] figure 8.

An assimilation of the boundary layer effects with that of obstacles having their displacement thicknesses, does not seem more or less justified in the case of lateral walls than in any other case and the critique in this case will be made on the approximations carried out to obtain a simple explicit formula.

3.3.2 - Approximations

In regard to the vortex schemes, the hypothesis common to references [2, 12, 13, 15], but discarded by S. Schneider [14] and according to which the vortex sheets localized in the boundary layers modify very little the circulation distribution on the span so that the free vortices in the potential flow are disregarded, is refuted by the computer results (figure 20). The integral differential equation for circulation distribution must be resolved (figure 21 and 22). Yet, this imperative becomes less obvious with fewer changes in corrections on the span as provided by Lazareff's scheme [15] (figure 23).

For those who allow for the schematization of boundary layer effects by lateral obstacles, there are two common approximations:

-a simplistic processing of the boundary layer development;

-the hypothesis of a uniform cross-flow.

The variations of δ_j is computed without the three-dimen-
sional effects, and in particular the corner effect. The lat-
ter is already quite significant in the angle of two plane
walls without gradient [18] and a fortiori root eddies appear-
ing in the absence of connection clearances between the wing
and wall [19], due in particular to lateral boundary layer
separations in the presence of the pressure gradient in the
vicinity of the stagnation point. Visualizations [20] dem-
onstrate the deformation of the parietal streamlines (figure
26), even over very slender obstacles.

These observations condemn the simplistic integration of
Karman's equation at δ_k and constant M. Assimilation of the
streamlines with lines parallel to the axis is also not very
realistic, but it does give (figure 27) results that are quite
close to a three-dimensional calculation [32], except in the
case of the separation which is provided only by the latter
(and which does not lead to a usable result).

The experimental points for the boundary layer soundings
(S3MA) are unfortunately too numerous to validate such cal-
culations which, moreover, do not account for the airfoil
field and the whirling eddies created at its root.

-The hypothesis of the transversal uniformity of the flow,
partially substantiated by certain experimental results (fig-
ure 1, 2, 3, 4) nevertheless appears only as an inadequate
approximation if we look at the shock forms (figure 5, 6).

In conclusion, it seems that the formulas established
with such dubious schematizations and such unsubstantiated
simplifications must be considered empirical and must be

16

carefully validated by systematic testing.

3.3.3 - Validations

Experiments were carried out for the purpose of validating the formulas derived from vortex schemes. It is hard to draw conclusions from them:

-Van den Berg [2] comparing the results of Mendelsohn and Polhamus [22] with Preston's formula wrote: "the theoretical results do not quite coincide with the experimental results. The main reason is probably due to a too simple hypothesis about the location of free vortices". This conclusion was adopted by Cambrink [4].

-Menard [12] used both pressure measurements in the median section of an HM 12 airfoil with a geometric aspect ratio of 1.3 and weightings along the entire wing (with a lateral clearance of 2 mm for a span of 780) and a boundary layer 13 to 16 mm thick, depending on the roughness of the collector.

The local correction of the angle of attack in the median plane applied to the pressure integral and the mean correction applied to the weightings are consistent and lead to a single curve $C_3(\alpha)$ representing the infinite aspect ratio.

In another experiment performed with a Clark Y airfoil of 18 % and a chord of 90 mm for two very different geometric aspect ratios (0.55 and 8.66), the pressures measured in the median plane (without lateral clearance) give, after corrections, lift gradients equal to about 1% $(\partial C_3/\partial\alpha = 0.1017$ and 0.103).

-Lavogiez and Dyment [23] also concluded the validity of the vortex scheme according to the $C_3(\alpha)$ curves obtained in

the presence of boundary layers under more or less suction.

-Heid and Stanislas [24] used a double exposure holo-
graphy which gives the complete field of the speed vectors
of the flow, in order to establish this validity. They con-
cluded that the value of the angle of attack correction, cal-
culated at the wing center, is satisfactory, but that the lon-
gitudinal variation of the angle induced on the test section
axis downstream from the airfoil and its variation in the med-
ian plane would agree more satisfactorily with the experiment
if the vortex system were placed at the tail quadrant of the
airfoil.

Calculation of the angle of attack corrrection at the
center is habitually completed by a lift correction if this
angle of attack correction exhibit; a longitudinal gradient.
Otherwise, a change in direction of the airfoil at zero lift,
associated with the curve induced by the longitudinal angle
of attack gradient, is taken into account approximatively by
computing the angle of attack correction, not at the center,
but at 3/4 from the airfoil chord, starting from the leading
edge [13].

Bernard Guelle's experiments [8, 9], were not carried out
to validate any particular formula, but were used a posteriori
by Barnwell [16] to justify his formula. However, there seems
to be an unexplainable difference between the factors of in-
fluence extracted from these tests (figure 25) and those that
we tried to deduce from Sugiyama's experiments [7].

One point from Bernard Guelle's experiments should, how-
ever, be brought to attention: when, for a given geometrical
angle of attack, he causes the lateral boundary layer thickness
to vary by suction, the representative points rigorously change
positions on the curves, whether it is for Lilienthal's polar

18

(figure 17) or for the stability curve (figure 18).

We may conclude from this not only that the effect is analogous to the angle of attack induced, but also that the longitudinal gradient of this correction must be small, otherwise it would introduce a generating camber variation of a moment independent from C_{ℓ} which would scatter the points outside the curve and a similar reasoning applies to the airfoil drag. Furthermore, until now, no one seemed to be concerned about the influence of a longitudinal speed gradient on the pressure drag of a region of the airfoil and on the resulting slipstream drag.

-Sugiyama [7] in his study of the effects of a clearance between wing and wall gives for this zero clearance the results presented in figure 11. It is delicate to use them quantitatively, because the boundary layer thicknesses provided are relative to a point situated at 1.5 c upstream from the airfoil, whereas the boundary layers at the leading edge were used to define k . Winter [26] using these results found much higher k values than Bernard-Guelle.

With such confusion in the experimental results, it is hard to pretend to validate schemes and formulas. We can only conclude that a more rigorous approach must be found. This might be possible by examining studies conducted on secondary flow in cascades, as quickly evoked below.

3.4 - Secondary Flows

If we simply consider a curved rectangular conduit (figure 28 extracted from [25]) whose horizontal walls have generated boundary layer profiles represented upstream, a secondary cross-flow is found downstream.

This appearance may be explained by schematizing the
boundary layer flow using vortices whose axes cross the flow
and which are situated near the walls. After deflecting, they
produce a nonzero longitudinal component without requiring a
variation of circulation on an absent airfoil. Introduction
of cascades or an airfoil to generate the deflection of the
flow fractionates these vortices, as shown by Winter [26], in
figures 29 and 30.

This phenomenon, fundamental in cascades with strong de-
flection, has received more attention in this case than in
airfoil tests: a recent work [25] does not contain less than
71 references on this subject. On this basis, the authors
proposed a much more sophisticated method than the preceding
ones and retained primarily the three-dimensional trait of
the secondary flow. Viscous layers are processed by integral
equations for the conservation of momentum with the inclusion
of entrainment in the form of Head [30] and accounting for the
secondary vorticity.

The develops that follow for the study of this secondary
flow are inspired in particular from the works of:

-Hawthorne [27]: introduction of a stream function from the
 secondary flow in a plane normal to the main flow.
-Mellor and Wood [28]: expressions uncoupled from the speed
 field satisfying the boundary conditions.
-Horlock [29]: solution in the form of products of functions.

They are not directly applicable to the case of an air-
foil alone. The experimental verification, in the case of
cascades [31], validates this approach satisfactorily enough
that this method can be recommended for investigations of air-
foils between walls. There are still local problems to be
solved: in particular, the leading edge separation gives rise
to a vortex ring tightly surrounding the airfoil and it is not

suitably represented by the superposition of a "sound" flow
and a boundary layer flow.

4 - FINAL REMARKS

The discrepancy in the experimental results of various
authors leads us to the conclusion that the complex development
ment of lateral boundary layers in the presence of an airfoil
prevents us from describing their effect by using only one   /14
characteristic, such as the displacement thickness of an
empty test section at the airfoil level.

The importance of three-dimensional effects, which ex-
tend way beyond the displacement thickness, is such that even
in the vicinity of the median plane, it is not obvious that
the flow is equivalent to a two-dimensional flow.

If per chance this were the case, determination of the
angle of attack induced, which seems to present very little
longitudinal gradient, demands an experimental study specific
to each installtation, as none of the models proposed appro-
priately accounts for all observations.

An improvement on the theoretical level requires a real-
istic view of the development of the boundary layers and of
the vortex systems based on visualizations and local measure-
ments, while handling at the same time the nonuniformity along
the span of the circulation distibutions outside the boundary
layer, due to secondary cross-flows in the presence of the
model.

The complexity of the theoretical operations required to
obtain sufficient knowledge of the corrections to be applied,
makes it necessary to perfect current methods of testing in
the plane stream while minimizing three-dimensional effects.

By controlling the lateral boundary layers, we can:

-avoid their premature separation in tests on lift
augmented airfoils;

-extrapolate the results within defined conditions of
variation up to the zero boundary layer.

Other solutions, less reliable, but also less costly
might be tried as a comparison: panels with variable dimen-
sions, thinning of the airfoil at the tips, localized boundary
layer traps.

All efforts must be encouraged, as the problem of three-
dimensional effects is far from being solved at the present
time.

22

REFERENCES

[1] Experimental data base for computer Program Assessment:
AGARD AR 138 (1979)

[2] J. H. PESTON
The interference on a wing spanning a closed tunnel arising
from the boundary layers on the side walls, with special
reference to the design of two-dimensional tunnels.
Rand M. No. 1924 (21/3/44).

[3] A. CAILLOU
Study of the lift of an airfoil covered by the boundary
layer of a contiguous plane wall (Etude de la portance d'un pro-
fil baigné par la couche limite d'une paroi plane contigue).
Nord Aviation ARA/NT/76/67, 13 Sept. 1967.

[4] H.A. DAMBRINK
Investigation of the 2-dimensionality of the flow around
a profile in the NLR transonic wind tunnel.
Private report by the author (1972).

[5] P. BOUVIER
Testing of a new method for boundary layer transition onset
on an aircraft model. (Essai d'une nouvelle méthode de
déclenchement de la transition de la couche limite sur une
maquette f'avion.) R.S.F. 1/788 GY (June 1981).

[6] S. OTSUKA, Y. SUGIYAMA
On the performance of a wing having tip clearance.
Part 1: The case in which the tip clearance is contained
within a nonuniform flow.
Memories Fac. Engineering, Nagoya University Vol. 2, No. 1,
May 1969.
Part 5: An experimental study of end wall boundary layers.
Bull. Japan Soc. of Mechanical Engineering, Vol. 18, No. 123,
Sept. 1975.

[7] Y. Sugiyama
Aerodynamic Characteristics of a rectangular wing with a
tip clearance in a channel.
Journ. of Applied Mechanics, Dec. 1977, pp. 541-547.

[8] R. BERNARD GUELLE
Influence of lateral boundary layers of a wind tunnel in
plane stream transonic tests (Influence des couches limites
latérales de soufflerie dans les essais transsoniques en
courant plan).

[9] R. BERNARD GUELLE, J. P. CHEVALLIER
Lateral boundary layer effects on two-dimensional tests.
48th STA Meeting, Toulouse, Sept. 1977.

[10] B. PORCHERON
Experimental study of flow past a lift augmented airfoil.
(Etude expérimentale de l'écoulement autour d'un profil
hypersustenté). R.S.F. 19/1736 AY. April 1981.

[11] W.L. COWLEY, G.A. McMILLAN
Pressure exploration over an aerofoil that completely spans a
wind tunnel.
R. and M. 1597.

[12] M. MENARD
Contribution to the aerodynamic study of the wing.
(Contribution à l'étude aérodynamique de l'aile et de
l'hélice). Doctorate thesis, Paris, 1950.

[13] J. BARBIEUX
Contribution to the study of the effect of a wall in plane,
incompressible flow. (Contribution à l'étude de l'effet de
paroi en écoulement plan incompressible). P.S.T. No. 304,
1955.

[14] S. SCHNEIDER
Effect of boundary layers on the plane flow. (Effet des couches
limites sur le courant plan). Note ONERA GSMA 108023 (1968).

[15] M. LAZAREFF
Correction of the lateral boundary layers. (Correction des
couches limites latérales).Note SNIAS A/ETP/A/181 564, (1976)

[16] R.W. BARNWELL
A similarity rule for compressibility and side wall boundary
layer effects in two-dimensional wind tunnels. AIAA 79-108.

[17] J. P. CHEVALLIER
Effect of lateral boundary layers in tests in plane flow.
(Effet des couches limites laterales dans les essais en
courant plan) R.S.F. 20/3075 AY 101 A, November 1980.

[18] D. ARNAL, J. COUSTEIX
Subsonic flow at the corner of two walls. (Ecoulement subsonique
dans l'angle de deux parois). 17e Colloque Aerodynamique
Appliquee, Grenoble, 1980.

[19] R.G. LEGENDRE
Groove at a wing root on a fuselage. (Congés à l'emplanture
d'une aile sur un fuselage). R.A. No. 1973-1, pp. 1-4.

[20] H. WERLE, M. GALLON
Chimney wakes, grid and turbomachine bundles, some visualization
examples based on hydraulic analogy. (Sillages de cheminées,
faisceaux tubulaires grilles et turbomachines. Quelques
examples de visualisations basés sur l'analogie hydraulique).
La Houille Blanche No. 4, 1973, pp. 339-360.

[21] B. Van den BERG
Some notes on two-dimensional high lift tests in wind tunnels.
NLR M.P. 70.008.

[22] R.A. MENDELSOHN, J.A. POLHAMUS
Effect of the tunnel wall boundary layer on test results of
a wing protruding from a tunnel wall. NACA TN 1244, 1947.

[23] A. LAVOGIEZ, A. DYMENT
Report on the correction of the effects of lateral walls in
plane, subsonic flow. (Note sur la correction des effets de
parois latérales en écoulement plan subsonique.
IMFL No. 76/04, Feb. 1976.

24

[24] G. HEID, M. STANISLAS
Double exposure holographic study of the tridimensional
nature of flow around a wing profile in a wind tunnel.
(Etude par holographie à double exposition du caractère bidimens
tridimensionnel de l'écoulement autour d'un profil d'aile en
soufflerie). IMFL No. 80/31 and 81/24.

[25] MMe J. CARO, A. COMTE, G. HALTER, L. LANDRIVON, F. LEBOEUR,
G. OHAYON, R.O. PAPAILLTOU
Study of secondary flow in cascades. (Etude des ecoulements
secondaires dans les grilles d'aubes). Final Report,
Contract DRME 75, 317, May 1978.

[26] K.G. WINTER, J.H.B. SMITH
A comment on the origin of endwall interference in wind tunnel
tests of aerofoils. Tech. Memo Aero 1816, Août 1979

[27] W.R. HAWTHORNE
Rotational flow through cascades: the components of
vorticity. Quat. Journ. of Mech. and Ap. Math. (VIII-3), 1955.

[28] G.R. MELLOR, G.M. WOOD
An axial compressor end wall boundary layer theory.
J. of Basic Engineering, 1971.

[29] HORLOCK
Cross-flows unbounded three-dimensional turbulent boundary
layers.
CUED/A TR 28, Cambridge University, 1976.

[30] M.R. HEAD
Entrainment approach
VKI Short Course on turbulent boundary layers, 1968.

[31] R. FLOT, K.D. PAPAILLIOU
Secondary Flow in cascades. (Ecoulements secondaires dans
les grilles d'aubes). Annual Report DRME, Contract 73/317.

[32] J. COUSTEIX
Theoretical analysis and prediction methods for the three-
dimensional turbulent boundary layer. (Analyse théorique et
moyens de prévision de la couche limite turbulente
tridimensionnelle). Publication ONERA 157, 1974.

24a
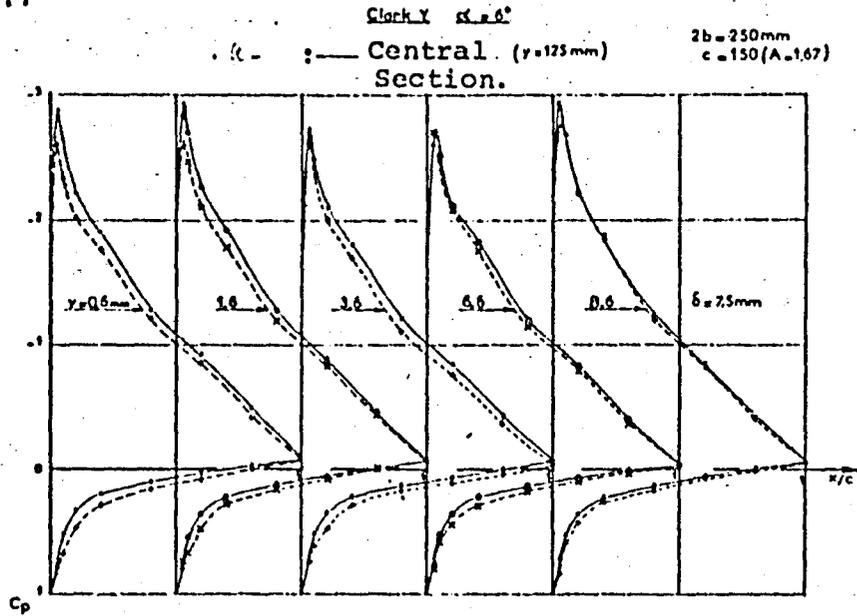
Figure 1 - Pressure Distributions Over Different
Sections of An Airfoil Covered By The
Parietal Boundary Layer [3].

Clark Y Air- 2b=250mm c=150mm(A=1,67)
foil.
$V_0 = 30$ m/s.
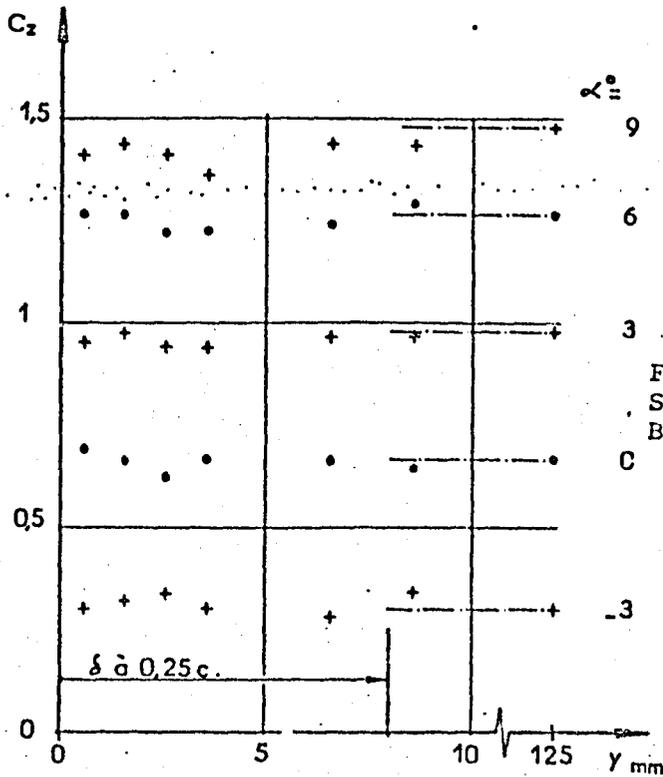
Figure 2- Local lift of The
Sections Covered By The Parietal
Boundary Layer [3].

M = 0.3 , α = 3,6 .
2b = 420mm
c = 180mm (A=2,33)
δ = 21mm

Central Section.

Wall of the Test Section.

-1

0

0,5

1

x/c

Cp
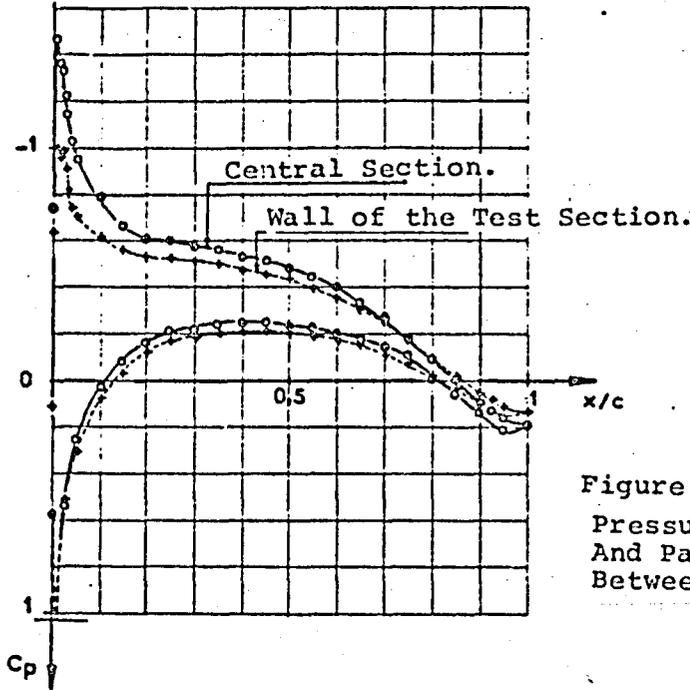
Figure 3

Pressure Distributions Over The Median
And Parietal Sections Of An Airfoil
Between Walls [4].

Distributions Over The Half-Span.

M = 0,3   α = 3,6 .

c = 180mm   2b = 420 mm. δ 21mm

C_z

($A=2,33$)

0,4

0,2

δ

0

0   0,5   1 $\frac{Y}{b}$
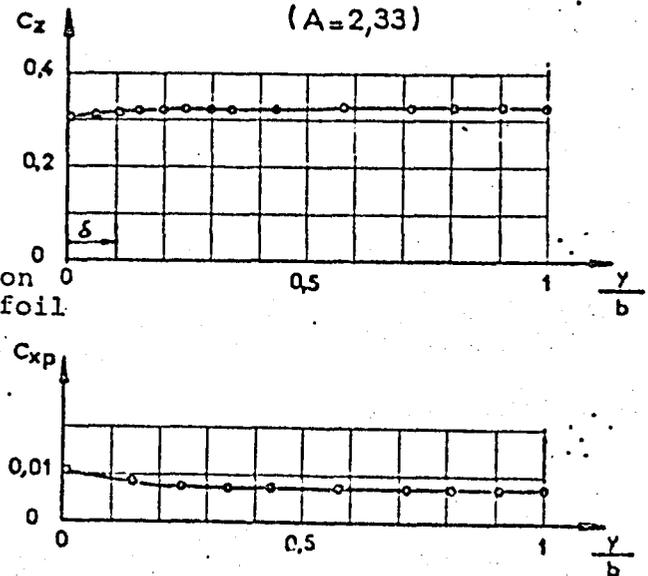
Figure 4

Lift And Resistance To Forward Motion
Of the Different Sections Of An Airfoil
Between Walls [4].

C_{xp}

0,01

0

0   0,5   1 $\frac{Y}{b}$

26

·Upper Surface.   M = 0,7   α = 3,6 .
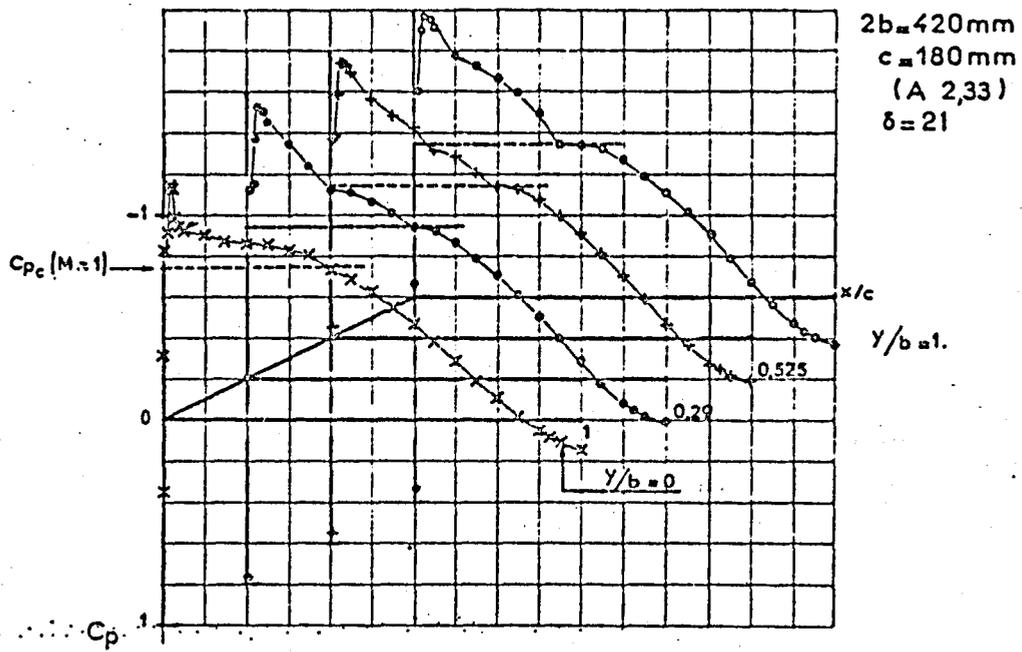
Figure 5 - Local Supersonic Flow Interferences On
The Upper Surface Of An Airfoil Between
Walls [4].

Natural
Transition

Band Not
Dislocated

Band Dislocated By 37°
Enlarged By 1 mm

Band Dislocated By 90°
Enlarged By 1 mm

Band Dislocated
By 37°

Carborundum
76 micrometers

Natural
Transition

S_3MA - Modern Airfoil
M_O = 0.74, alpha = 2°59
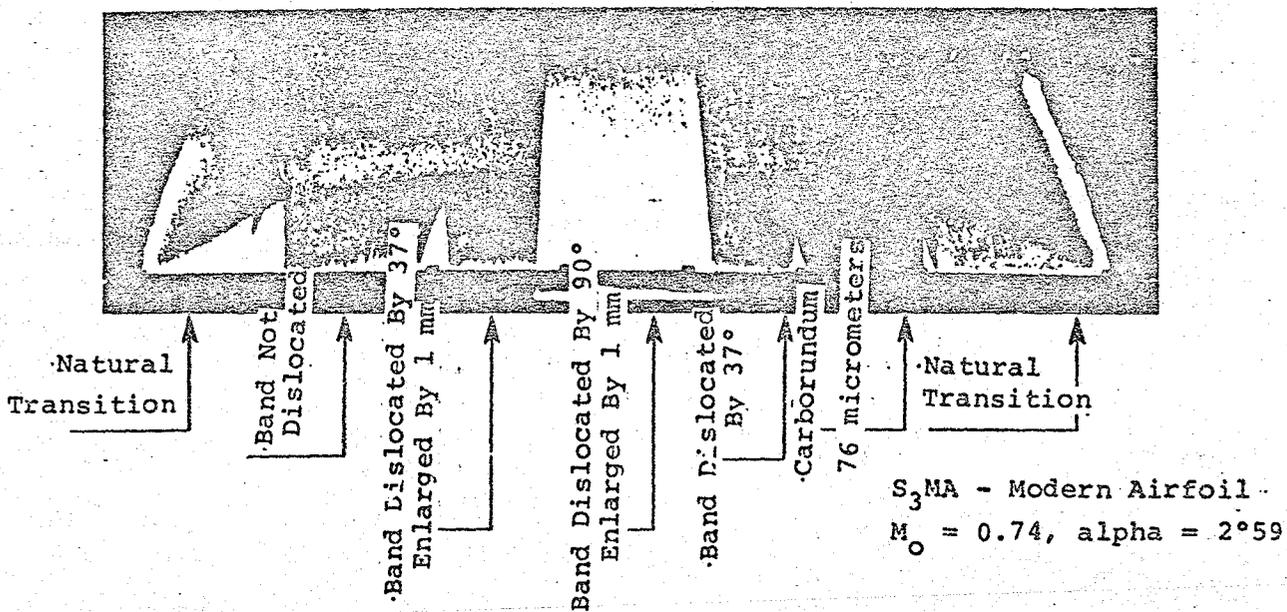
Figure 6 - Visualizations Over the Upper Surface Of
Three-Dimensional Effects At Mo = 0.74
And Alpha = 2.59° On A Modern Airfoil
[5].
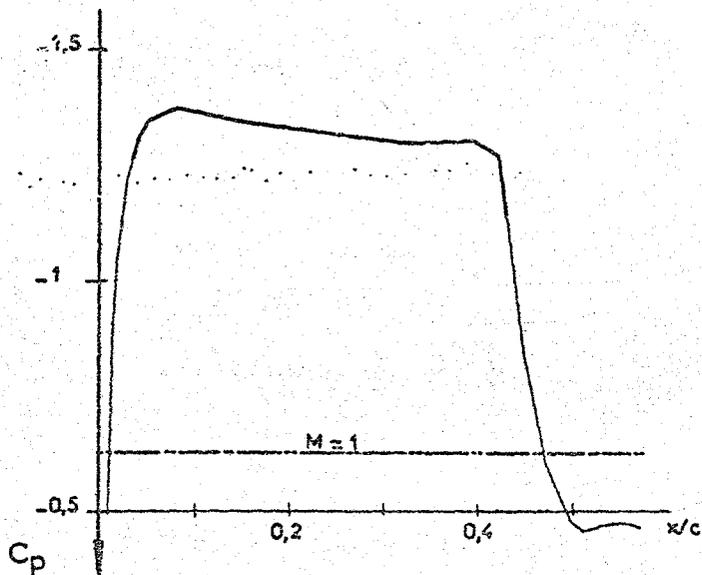
Figure 7 - Corresponding Pressure Distribution [5].

RAF 6 Airfoil $\alpha = 3°$
    c.70
    2b.300
     (A.4,28)
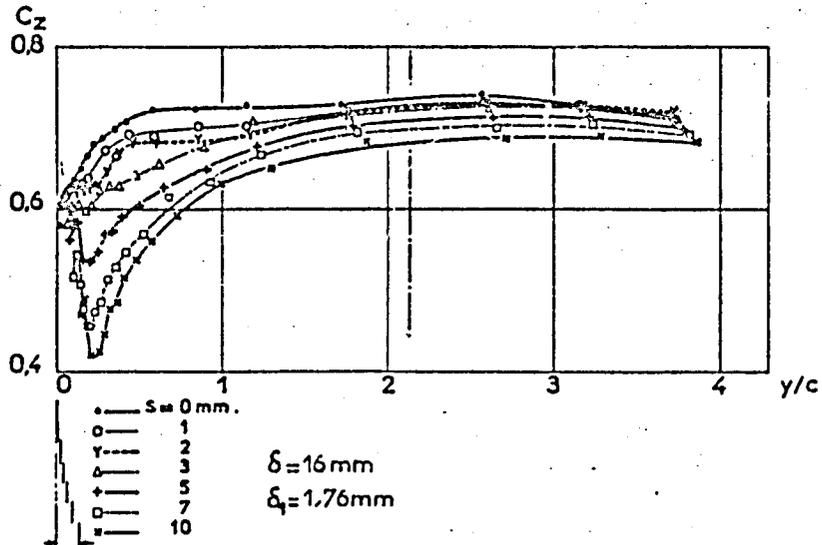
Figure 8 - Effect Of a Clearance Betwen Airfoil and
Wall On Local Lifts [6].

RAF 6 Airfoil

2b.300mm
   c.70mm
    (A 4,28)

$\alpha = 6°$
$R_e = 140000$
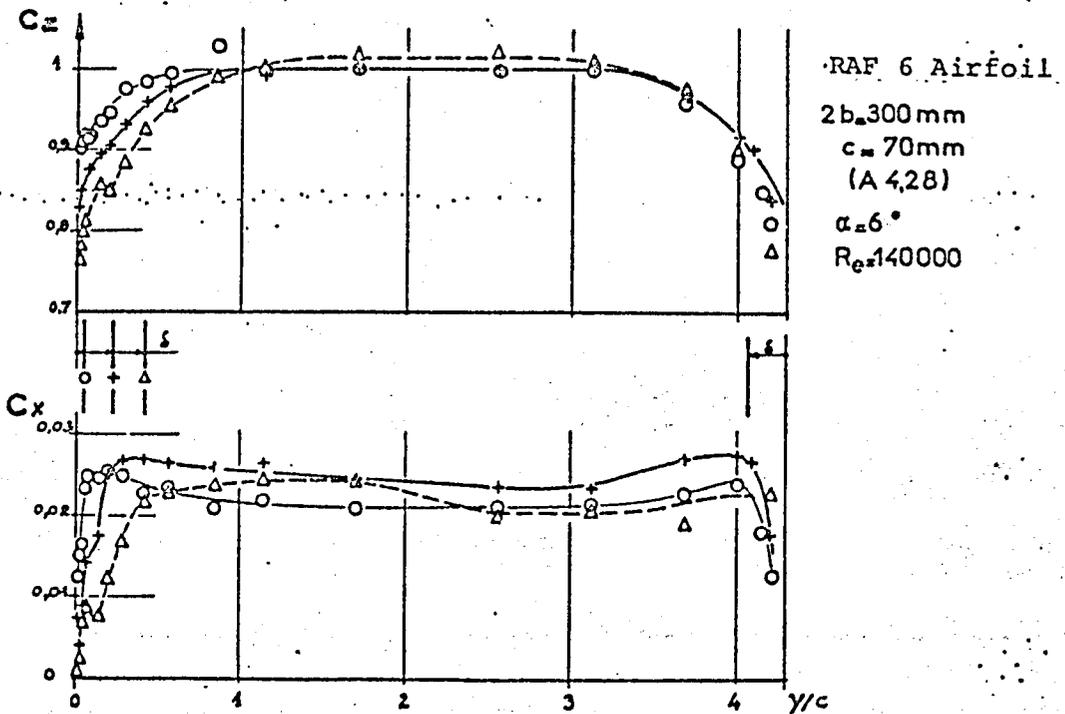
Figure 9 - Distributions of C_z and C_x Along the Span
For Different Boundary Layer Thicknesses [6].

29
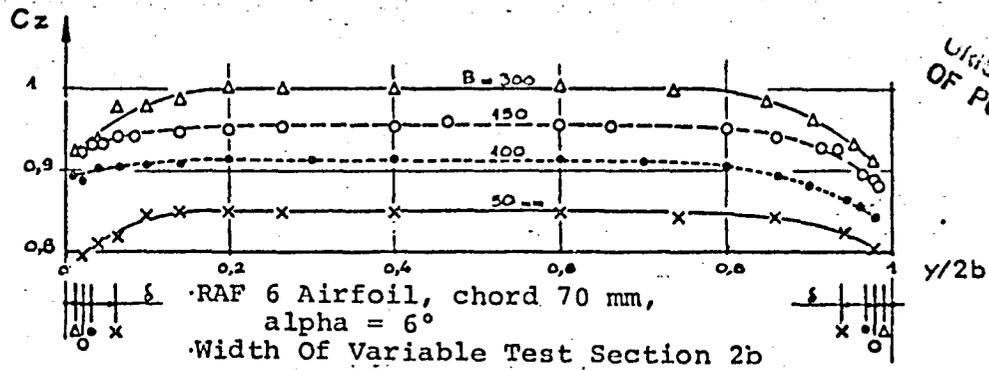
Figure 10 - Distributions of C_z Along A Variable Span
At A Given Boundary Layer [7].

·RAF 6 Airfoil, chord 70 mm,
alpha = 6°
·Width Of Variable Test Section 2b

Figure 11- Variation of the
Lift of the Median Section
As A Function of the Boundary
·Layer Thickness.
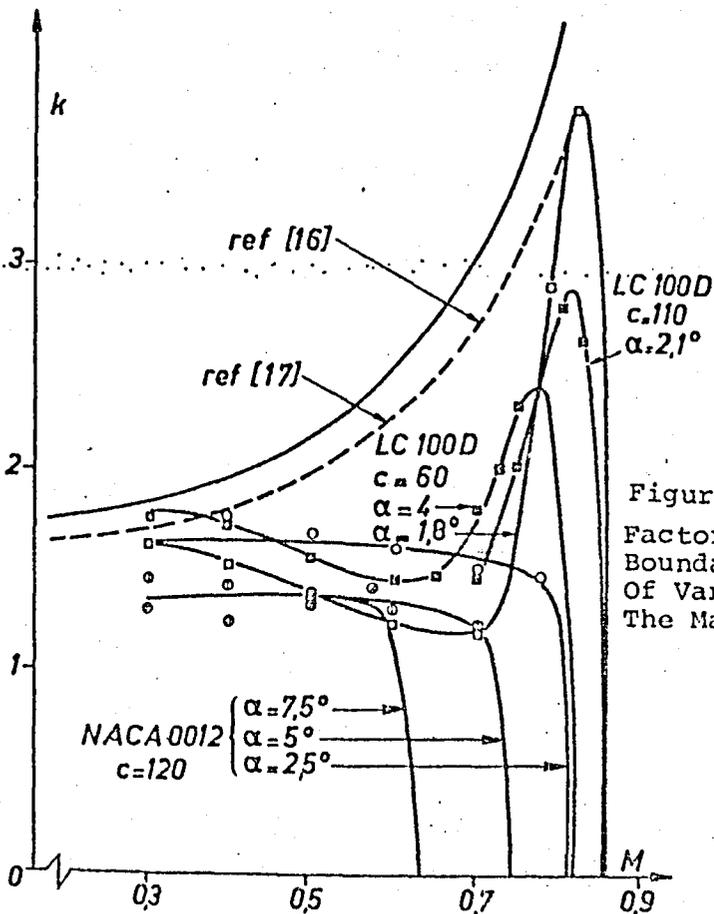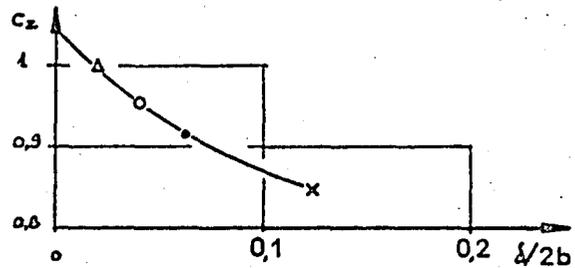
Figure 12

Factor Of Influence Of the Lateral
Boundary Layers In The Median Plane
Of Various Models As a Function Of
The Mach Number.

LC 100D
c.110
α.2,1°

ref [16]

ref [17]

LC 100D
c.60
α=4
α.1,8°

NACA 0012
c=120
α=7,5°
α=5°
α=2,5°

WITHOUT SUCTION

WITH SUCTION

α 12°

α 14°

α 16°

α 18°
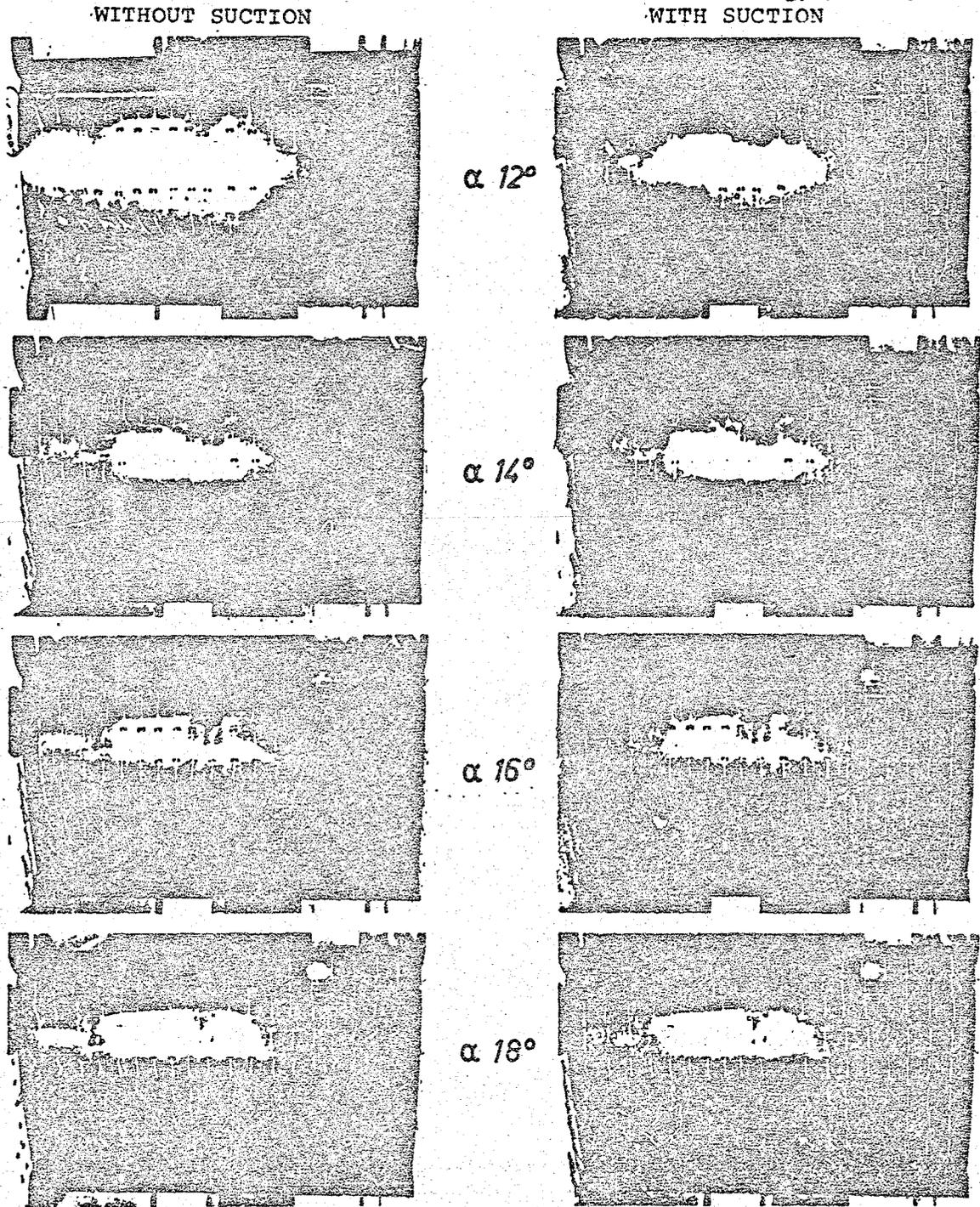
Figure 13 - Visualization, Using Strands Of Wool, Of
The upper Surface Of A Lift Augmented Airfoil
With and Without Control Of the Lateral Bound-
ary Layers.

31
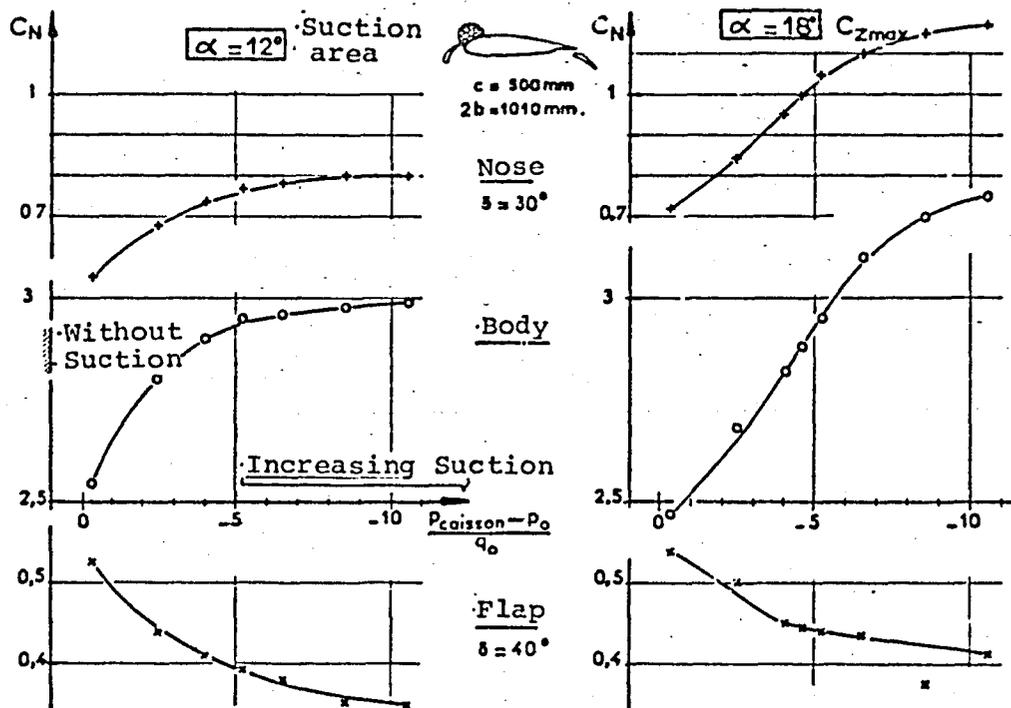
Figure 14 – Variation of the Normal Force Coefficients Of
the Elements Of A Lift Augmenting Airfoil As
A Function Of the Suction Rate of the Lateral
Boundary Layers.
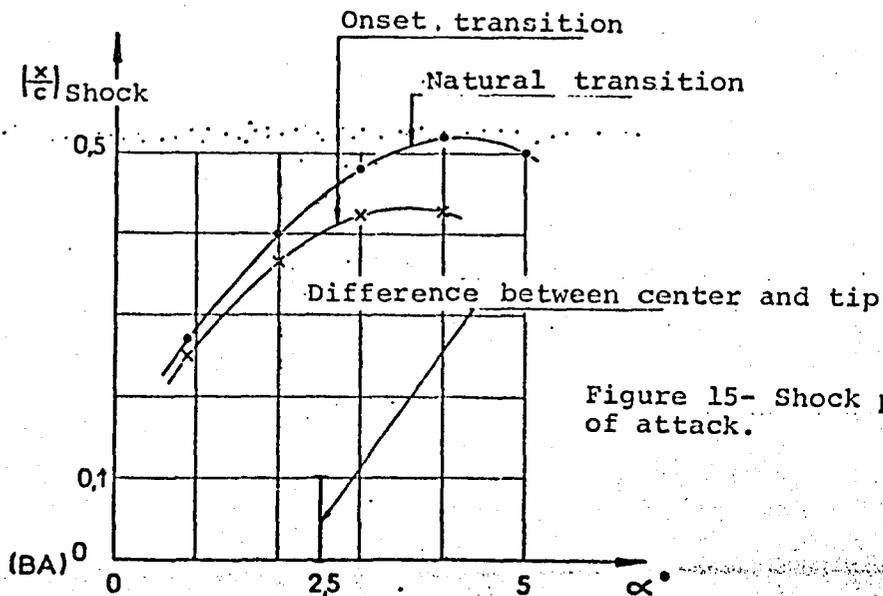
Figure 15– Shock position as a function
of attack.

2b=560
c=210 A=2,66

Modern Airfoil M = 0.74

NACA 12

$$\left(\frac{\Delta C_N}{C_N}\right)_{\alpha = c^{ste}}$$

M = 0,325 R_e = 3,5 10^6.

2b=60 c=120 A=0,66

$(\delta_1)BA$
b
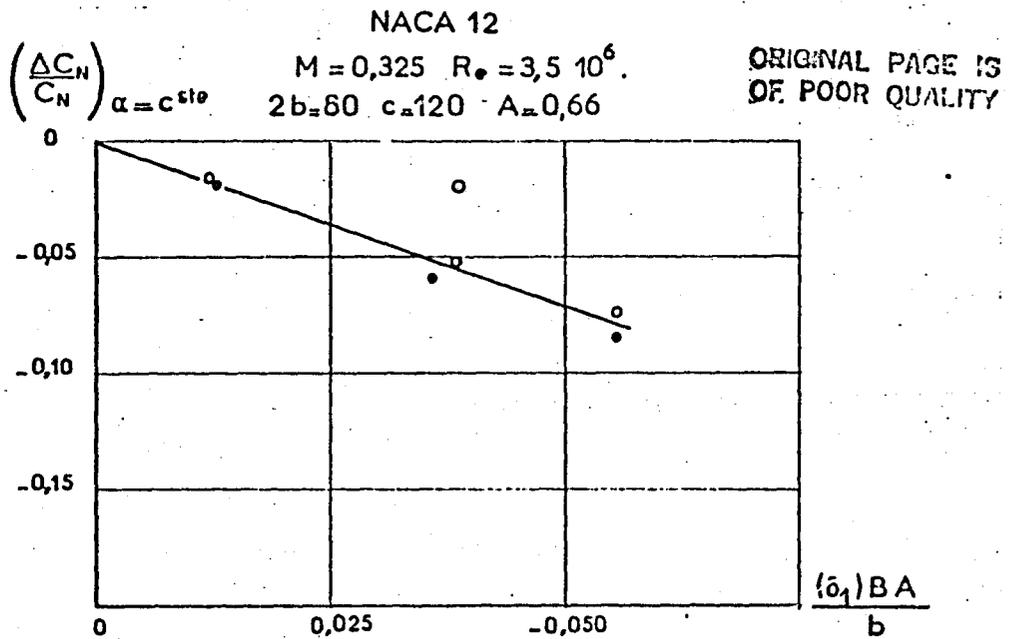
Figure 16 – Extrapolation Of the Normal Force Coefficient
In Zero Boundary Layer Conditions [8].

NACA 12 Airfoil c = 120 mm 2b = 80 mm.
Full Walls M_0 = 0,325   R = 3,5 10^6.
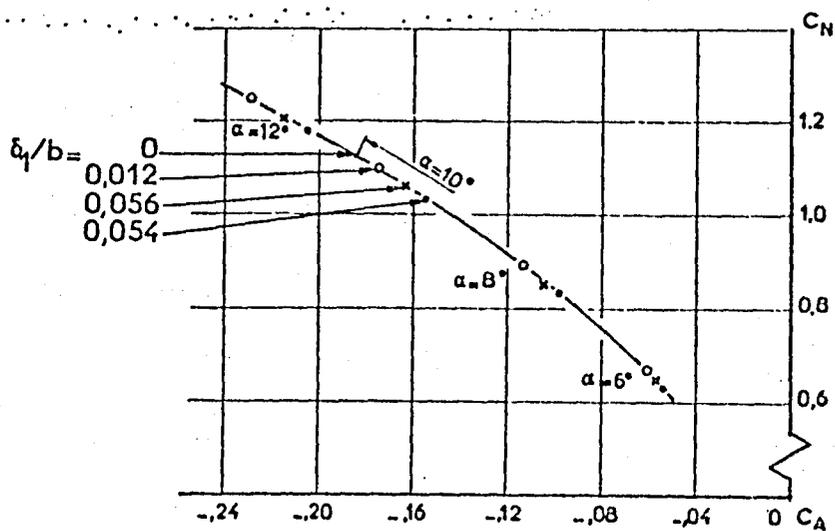
Figure 17 – Lilienthal's Polar Based On The Pressure
Integrations Over the Median Section Of
A NACA 12 Airfoil [8].

Influence Of the Lateral Boundary Layer

NACA12

$M = 0,325$

$R_e = 3,5 \ 10^6$

δ_{1DA}/b

- 0,054
x 0,036
○ 0,012
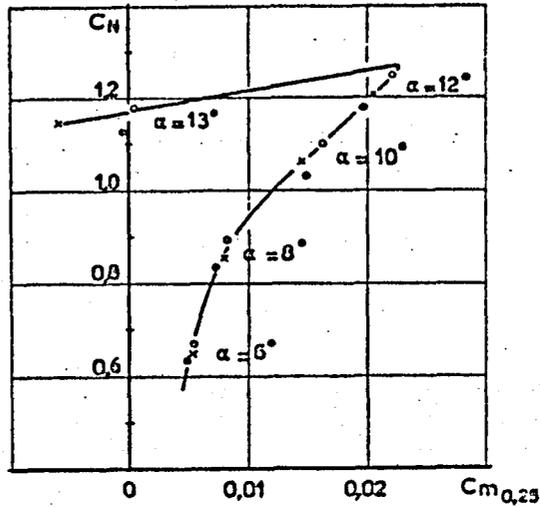
Figure 18 - Stability Curve, Based On The Pressure
Integrations Over the Median Section Of
A NACA 12 Airfoil [8].
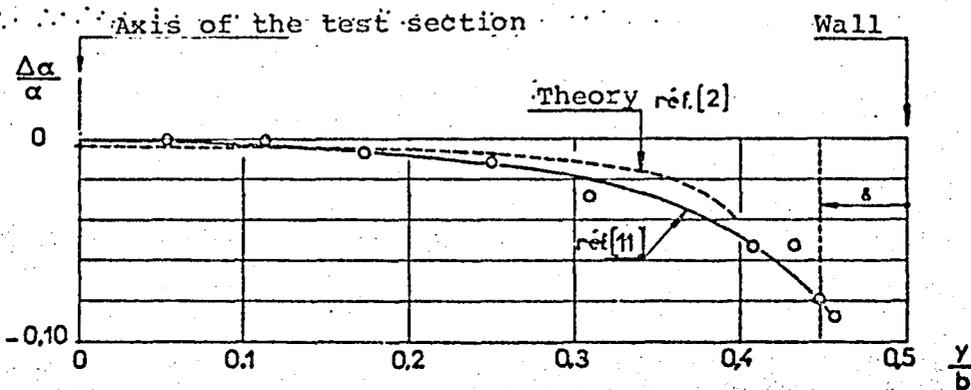
Figure 19 - Distribution Of the Rise Induced Along The
Span By Marginal Vortices And Their First
Image [2, 11].

34

Distribution of the induced
theoretical angle.

c = 90 mm
2b = 50 mm
A = 0,55 mm
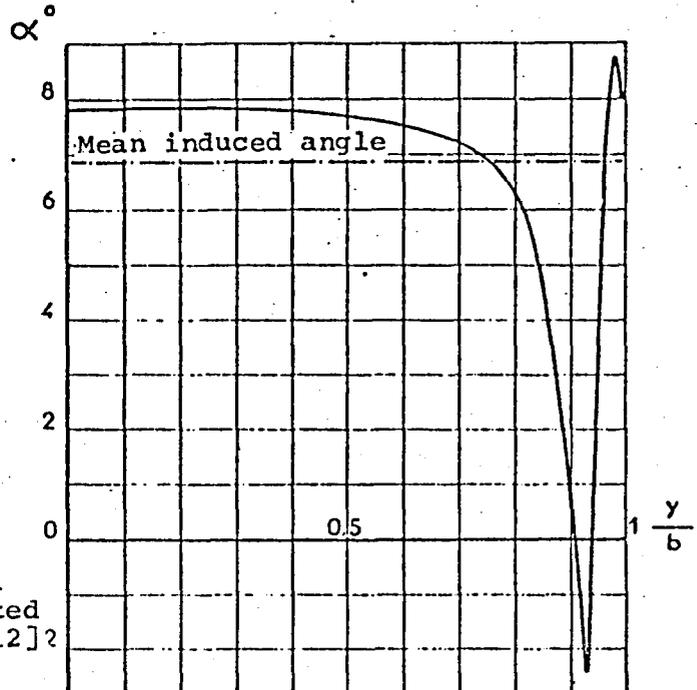
Figure 20- Distribution
Along The Span Of The
Rise Induced By Marginal
Vortices And The Unlimited
Queue Of Their Images [12]?

Mean induced angle

Variation of the rise along the span

2b=560 mm
c=210 mm} A = 2.66

$\frac{\delta_1}{b}$ = 0.015

ref. [12]

ref. [14]
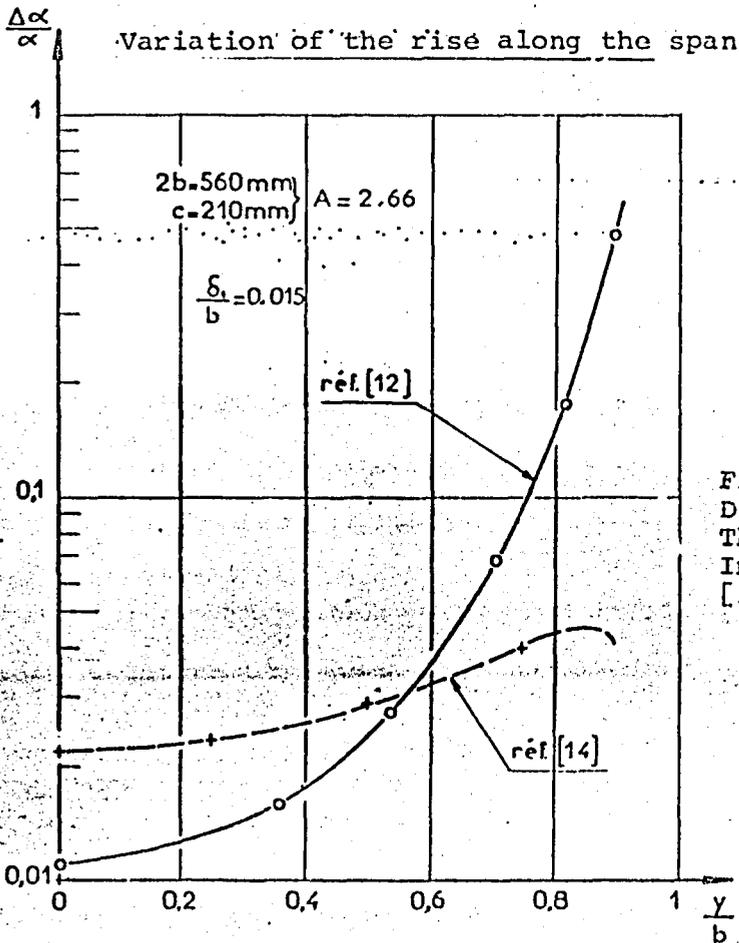
Figure 21- Comparative.
Distributions of the Rise Along
The Span With And Without
Including The Induced Effects
[12, 14].

VARIATION OF THE RELATIVE RISE

$$\frac{\Delta\alpha}{\alpha}$$

2b.560mm
c.210mm (A = 2,66)
$\delta_1/b = 0,015$

réf.[14]

réf.[12]
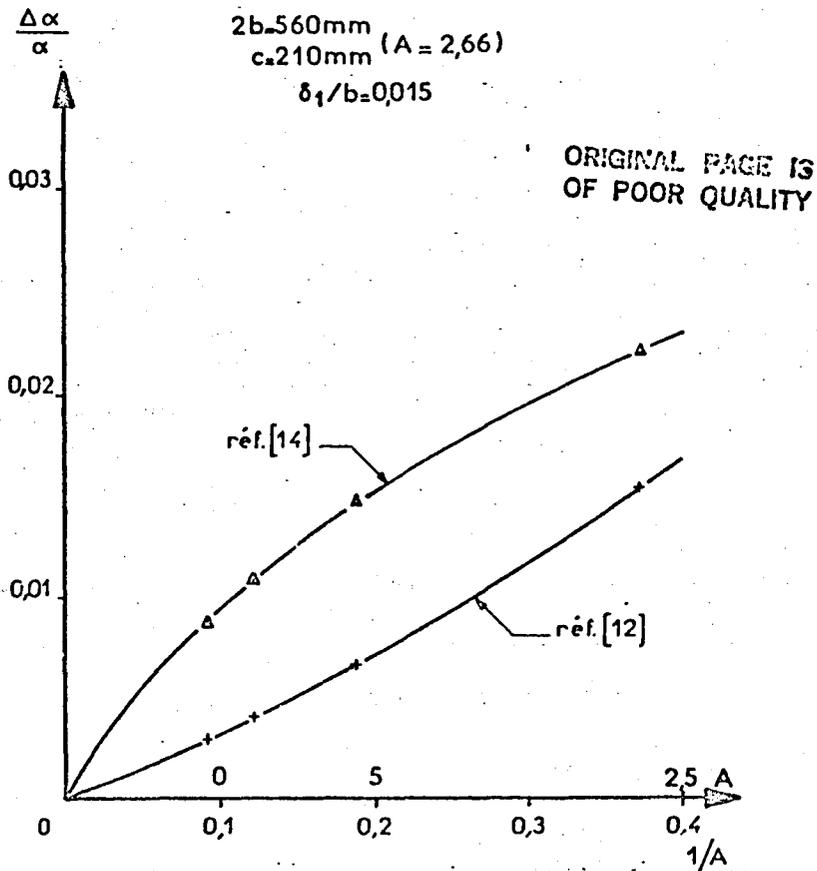
Figure 22 - Variation Of The Aspect Ratio Of The Rise
Induced In the Median Plane [1; 14].

$- \Delta Cz$

Initial Scheme

Modified Scheme

-b   0   + b
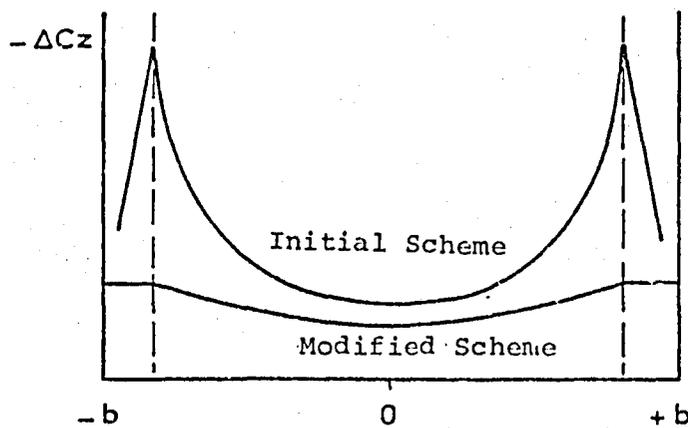
Figure 23 - Lift Corrections Along The Span Due To
Free Vortices Issuing From The Lifting
Line Or From the Trailing Edge [15].

36

$$k = \frac{\Delta\alpha}{\alpha} \cdot \frac{b}{\delta_1}$$

FACTOR OF INFLUENCE AS A FUNCTION OF THE ASPECT RATIO.

[12] [2]

réf [17]

$\delta_1/b = 0,015$ LC 100 A

réf [16] { $\delta_1/b = 0,05$ LC 100 D   c = 110

c = 60

NACA 012
c = 120

réf [14]

3

2

1

2   1   A

0   0,5   1   1/A

Figure 24- Variation of the
Factors Of Influence Based
On Various Improvements, As
A Function Of The Aspect
Ratio [12, 14, 16, 17].

$$k = \frac{\Delta\alpha}{\alpha} \cdot \frac{b}{h_s}$$

FACTOR OF INFLUENCE AS A FUNCTION
THE RELATIVE THICKNESS OF THE BOUNDARY
LAYER.

10

réf [7]

réf [12]

réf [24]

5

Figure 25

Variation Of the Factors Of Influence As A
Function Of the Relative Thickness of The
Boundary Layer.

réf [17]

réf [16]

réf [9]

1

0   0,02   0,04   0,06 $\frac{\delta_1}{b}$

37
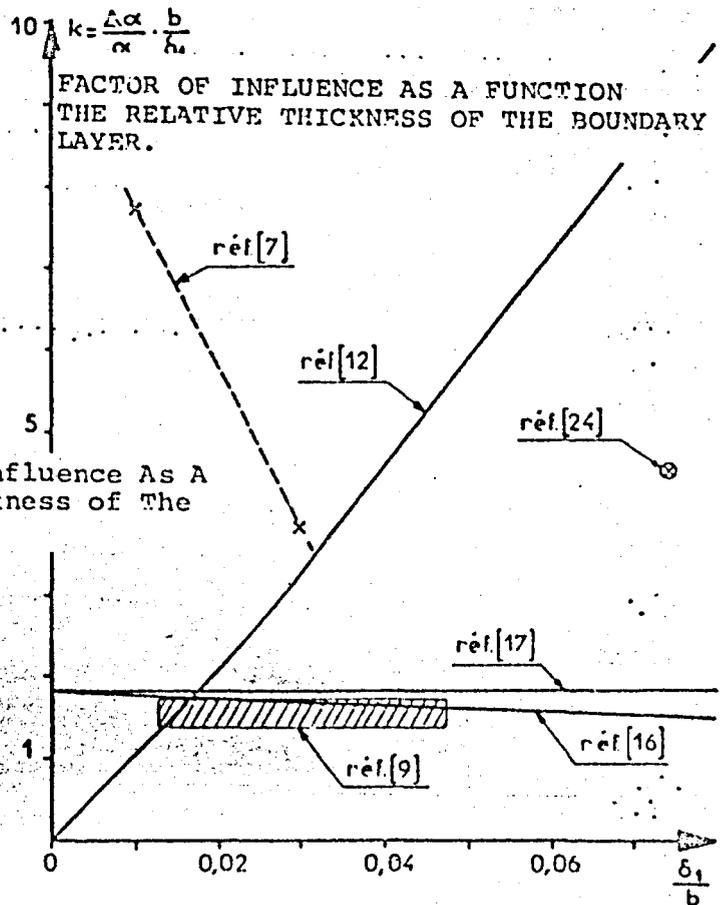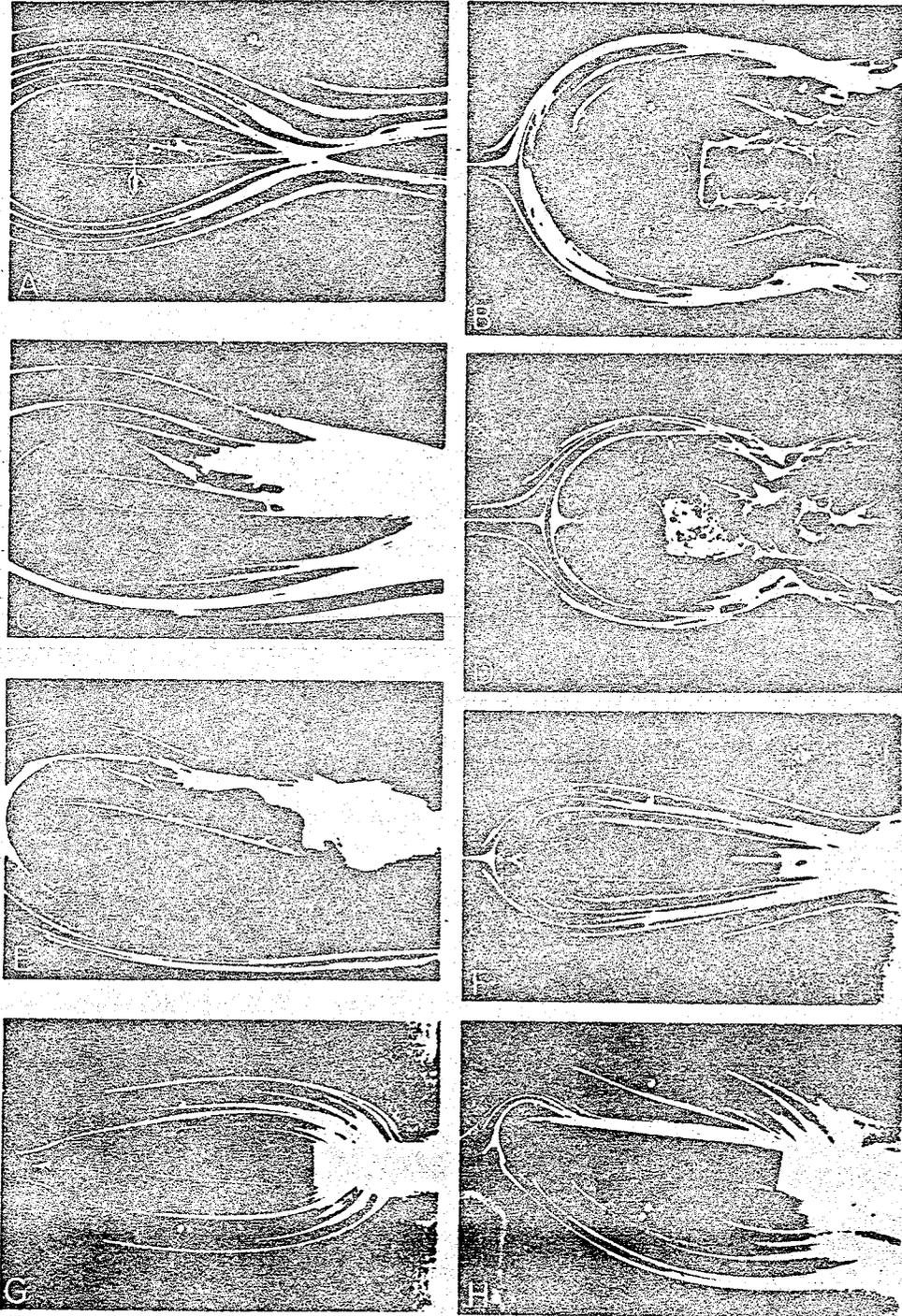
FIG. 26 – Streamlines In the Vicinity Of A Wall Upon
Which Various Obstacles Are Attached.
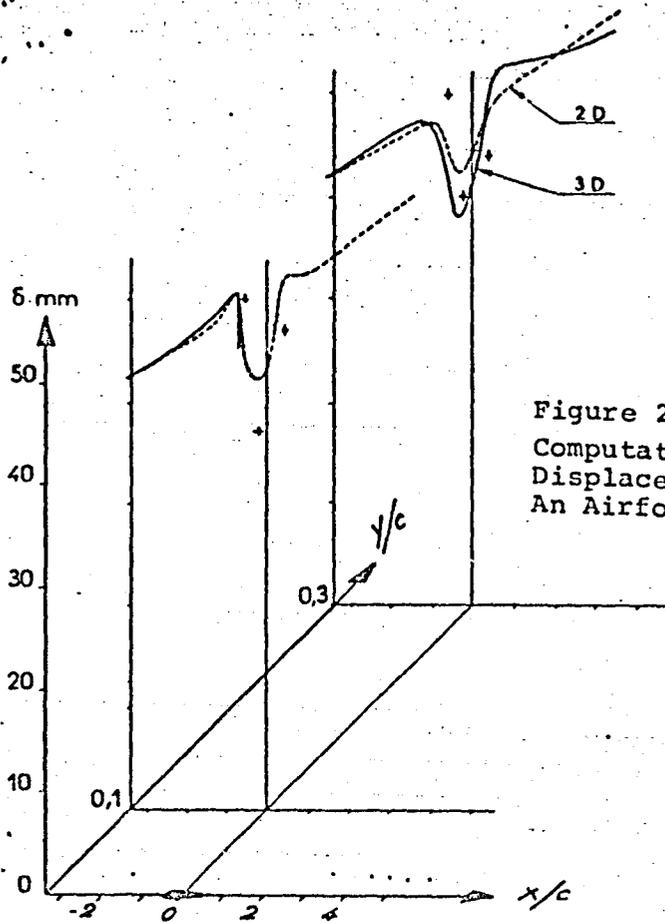
Figure 27

Computations of The Lateral Boundary Layer
Displacement Thickness On Two Lines Near
An Airfoil.
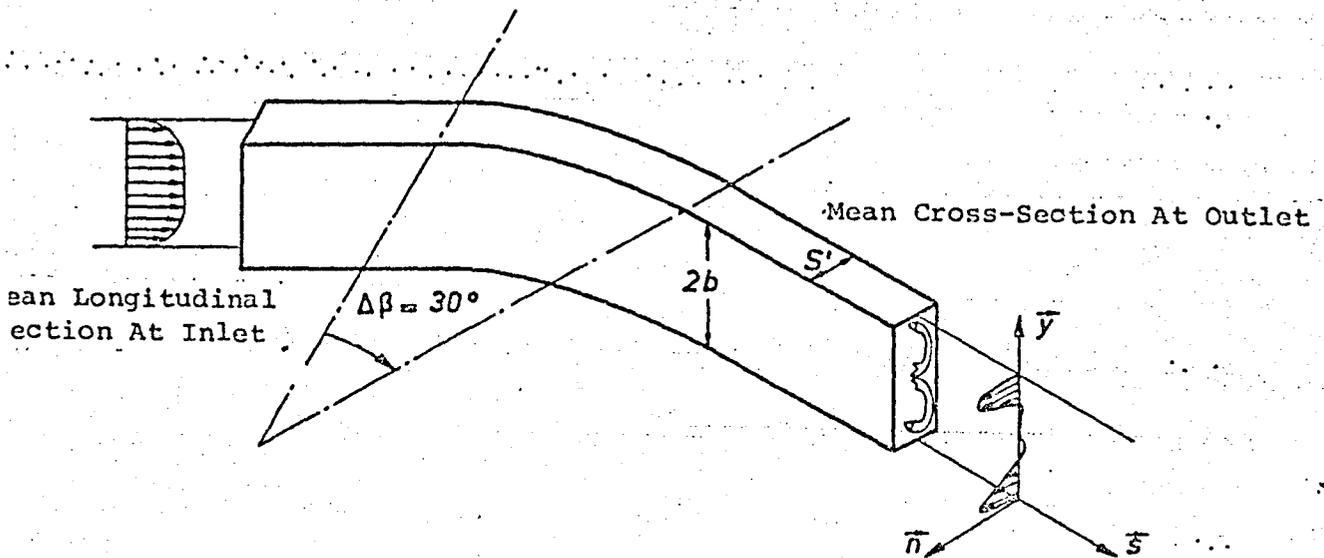
Figure 28 - Secondary Vorticity Created By The Deflection
Of Boundary Layer Vortices [25] In A Curved
Conduit.
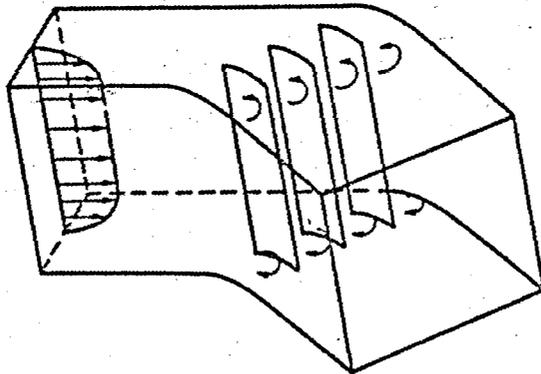
Figure 29 - Secondary Vorticity In Cascades.
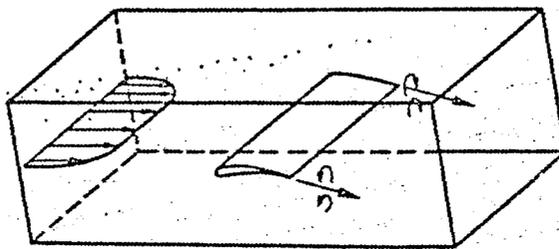
Figure 30 - Secondary Vorticity Upstream From An Airfoil.

40

End of Document